CLOUD PREDICTION EXPERIMENTS WITH THE LMD GCM

H. Le Treut
Laboratoire de Météorologie Dynamique
24, rue Lhomond, 75231 Paris Cedex 05, France

1. INTRODUCTION

The purpose of this paper is to describe the studies which have been done with the LMD GCM in order to develop new parameterizations of the cloud cover.

The LMD GCM has been described elsewhere (Sadourny and Laval, 1984). Let us only recall here that in its usual version the cloud cover is predicted with a scheme based on the assumption that cloudiness occurs whenever and wherever there is precipitation. This parameterization simulates reasonably well the cloud patterns associated with the intertropical convective regions and with the cyclonic areas in mid-latitudes (Le Treut and Laval, 1984). Yet it may be criticized for various reasons. First of all, an obvious unrealistic feature of the simulated cloudiness is the non-prediction of the stratus and stratocumulus clouds, at subtropical latitudes in the eastern part of the ocean basins, or at high latitudes, especially in the Summer Hemisphere. A scheme to predict those clouds in our model will be discussed in Section 2. The results of a 50 days simulation of the July climate are shown. It allows us to estimate the impact of the stratus and stratocumulus clouds on the general circulation. It is hard, due to the weak accuracy of the existing cloud climatologies, to make further criticism of the original model on the basis of its lack of realism. But it is possible to try to remove some of the physical simplifications which are assumed in it and to estimate the impact of these simplifications on the simulated cloudiness. In section 3 we will present some results of a statistical approach which allows non-convective precipitation and therefore non-convective cloudiness

to occur before the complete saturation of the gridbox. In Section 4 we will describe the first developments of a project which aims at predicting the cloud liquid water content as a new variable of the model.

2. PREDICTION OF THE STRATUS CLOUDS ; THEIR IMPACT ON THE SIMULATED CLIMATE

2.1 Definition

Detailed modelling of the stratocumulus clouds has been an active research field since the work of Lilly (1968) and their prediction in a GCM has been the object of various studies (Suarez et al,(1983), Slingo(1980), Ramanathan and Dickinson (1980)). All those parameterizations are crucially dependant on the representation of the planetary boundary layer.

In the LMD GCM the PBL is constituted by the four lower layers of the model, the top of which are respectively at the levels $\sigma = .979$, $\sigma = .941$, $\sigma = .873$ and $\sigma = .770$. The vertical turbulent eddy transport of momentum, heat and moisture is parameterized within those four layers using a turbulent eddy diffusion coefficient. This coefficient is chosen to decrease linearly with height, so that it becomes zero at the top of the boundary layer and is a function of the turbulent kinetic energy, itself diagnosed from the vertical stability and from the wind shear.

In order to define a representation of the boundary layer clouds we examined the large scale distribution of the parameters simulated by the model which could be used as a predictor : the relative humidity, the height of the Lifting Condensation Level and the stability coefficients S_n defined by

$$S_n = \frac{\delta_z s}{\frac{R\bar{T}}{P}\,\delta_z P}$$

where n is an index for the layer, $\delta_z s$ is the vertical increment of dry static energy, $\bar{T}$ is the mean temperature of the layer, P is the pressure, R the ideal gas constant and $\delta_z P$ the vertical increment of pressure. S_n is negative in unstable conditions; it then becomes positive in stable or conditionally unstable conditions, and reaches 1 when there is a temperature inversion. We chose to predict cloudiness, in conditions where the LCL was under the top of the PBL (a requirement almost always met in our model) and when the top of the PBL was not conditionally unstable, as an increasing function of the stability coefficient at the top of the PBL and a decreasing function of the stability coefficient at its bottom. The exact formulation is somewhat arbitrary and was chosen as follows.

$$f = \text{Min}\ (\text{Max}(S_3, S_4), 1.) * (1 - (\text{Min}(S_1, 1))^2)$$

Relative humidity was not found to be a useful predictor for the PBL clouds in our model.

2.2 Simulation of the July climate

Two 50-days simulations of the July climate have been done; the first one, referenced as "control" (CO) predicting only the precipitating clouds, and the second one, referenced as "stratus" (STR) predicting also the stratus and stratocumulus clouds. Both simulations start from the 11th of June 1979.

We present in Figure 1a,b,c the low, middle, and high cloudiness simulated in the STR case on the 12th of June 1979, and in Figure 2 the low cloudiness simulated on the same day in the CO case (middle and high cloudiness is unchanged between the two experiments). There is a clear increase of the low level cloudiness due to the prediction of the stratus clouds. It appears to be well located (on the Eastern side of the ocean basin, in the Artic or near 65°S).

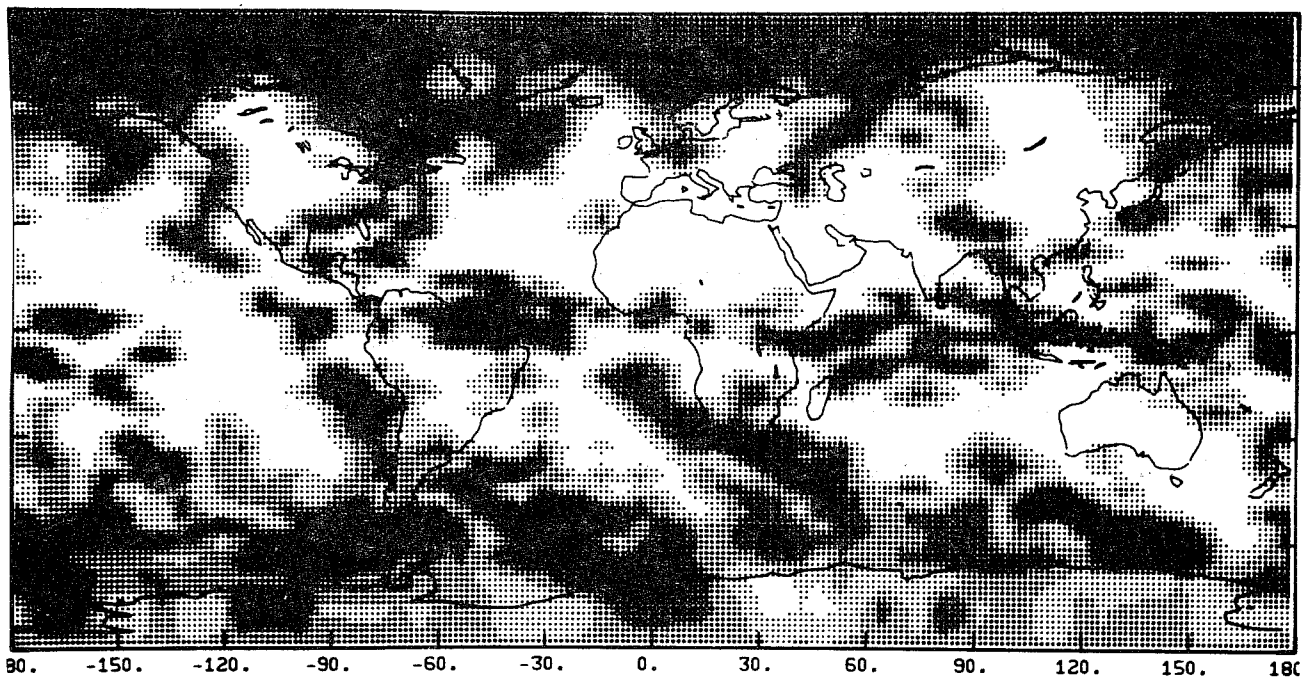

Figure 1,a: Low cloudiness on the 12th of June 79
(STR experiment)

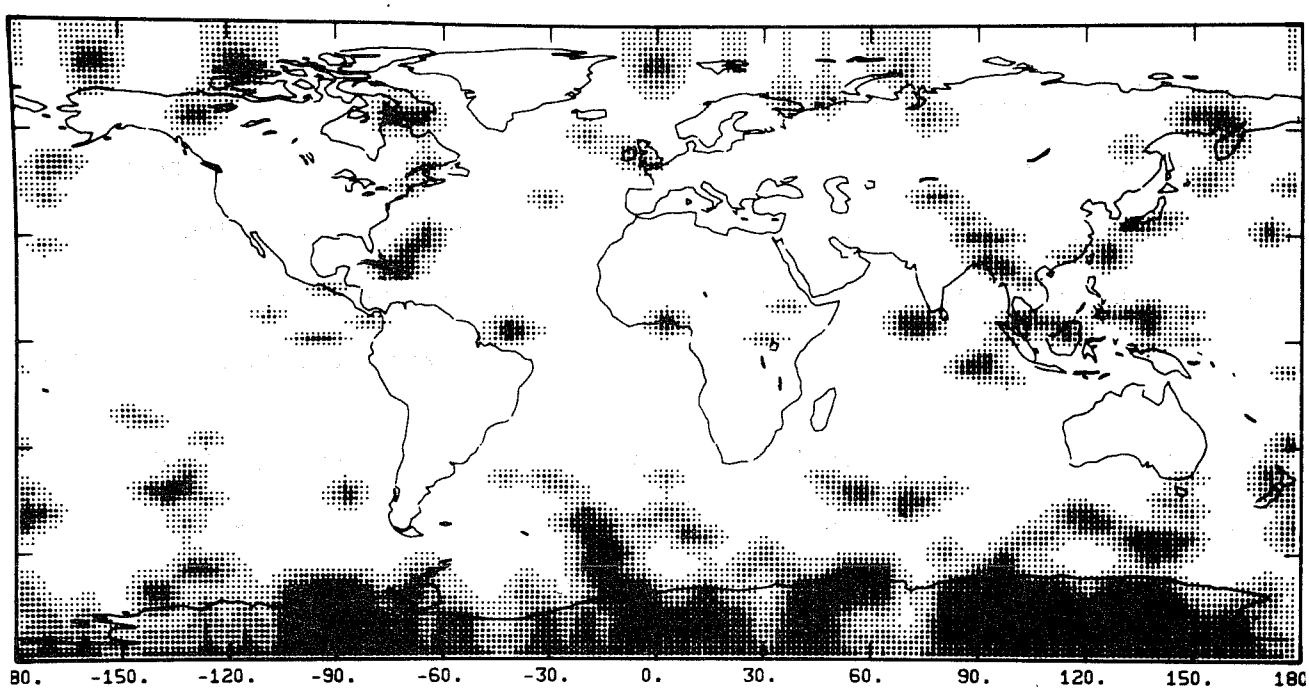

Figure 1,b: Middle level cloudiness on the 12th of June 79
(STR experiment)

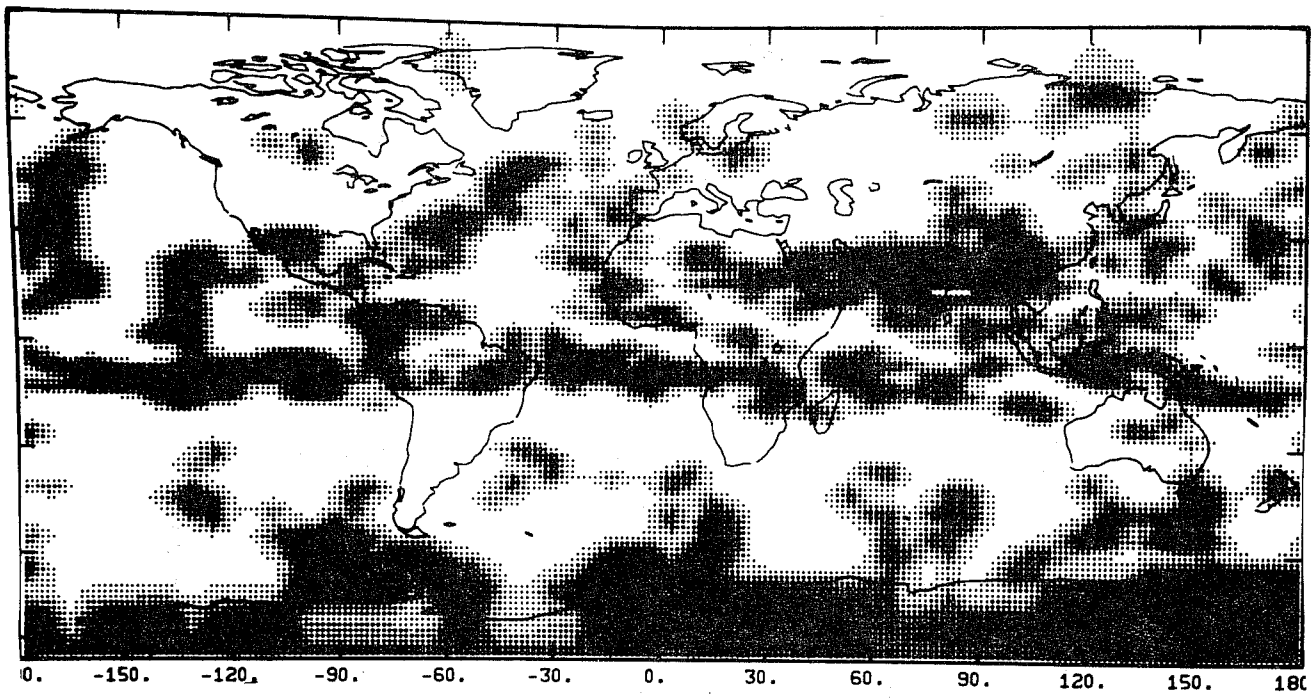

Figure 1,c: High cloudiness on the 12th of June 79
(STR experiment)

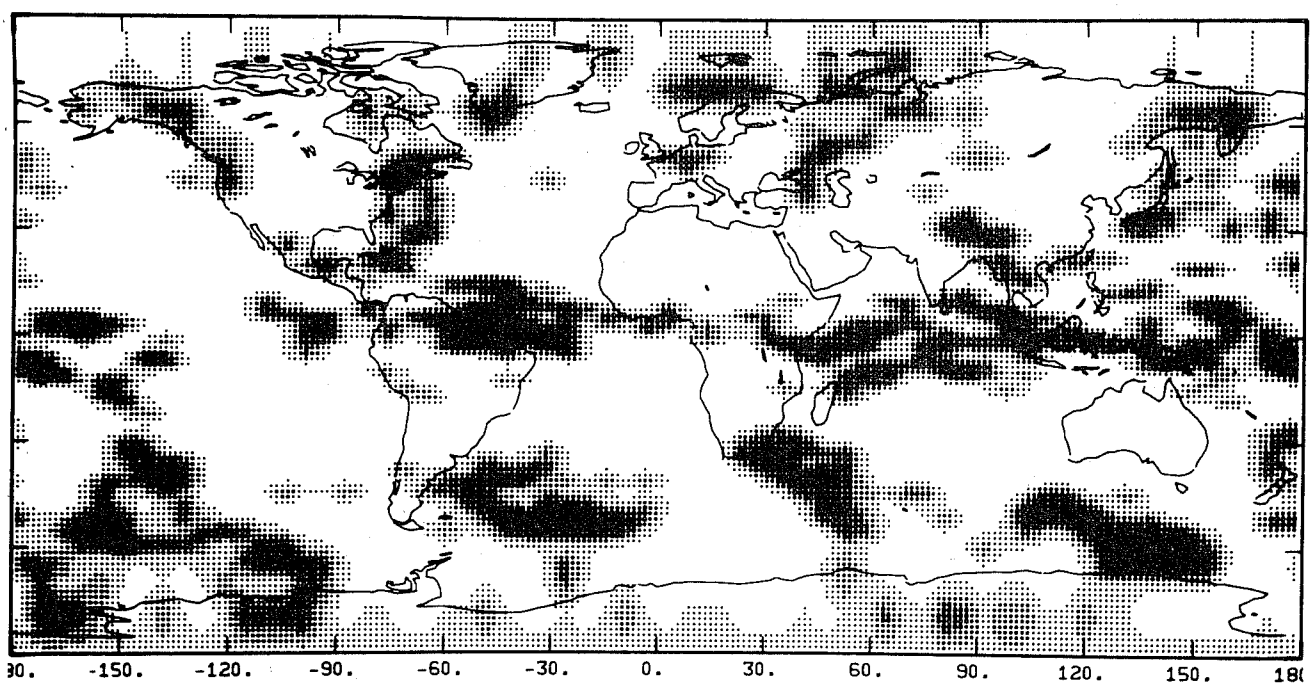

Figure 2 : Low cloudiness on the 12th of June 79
(CO experiment)

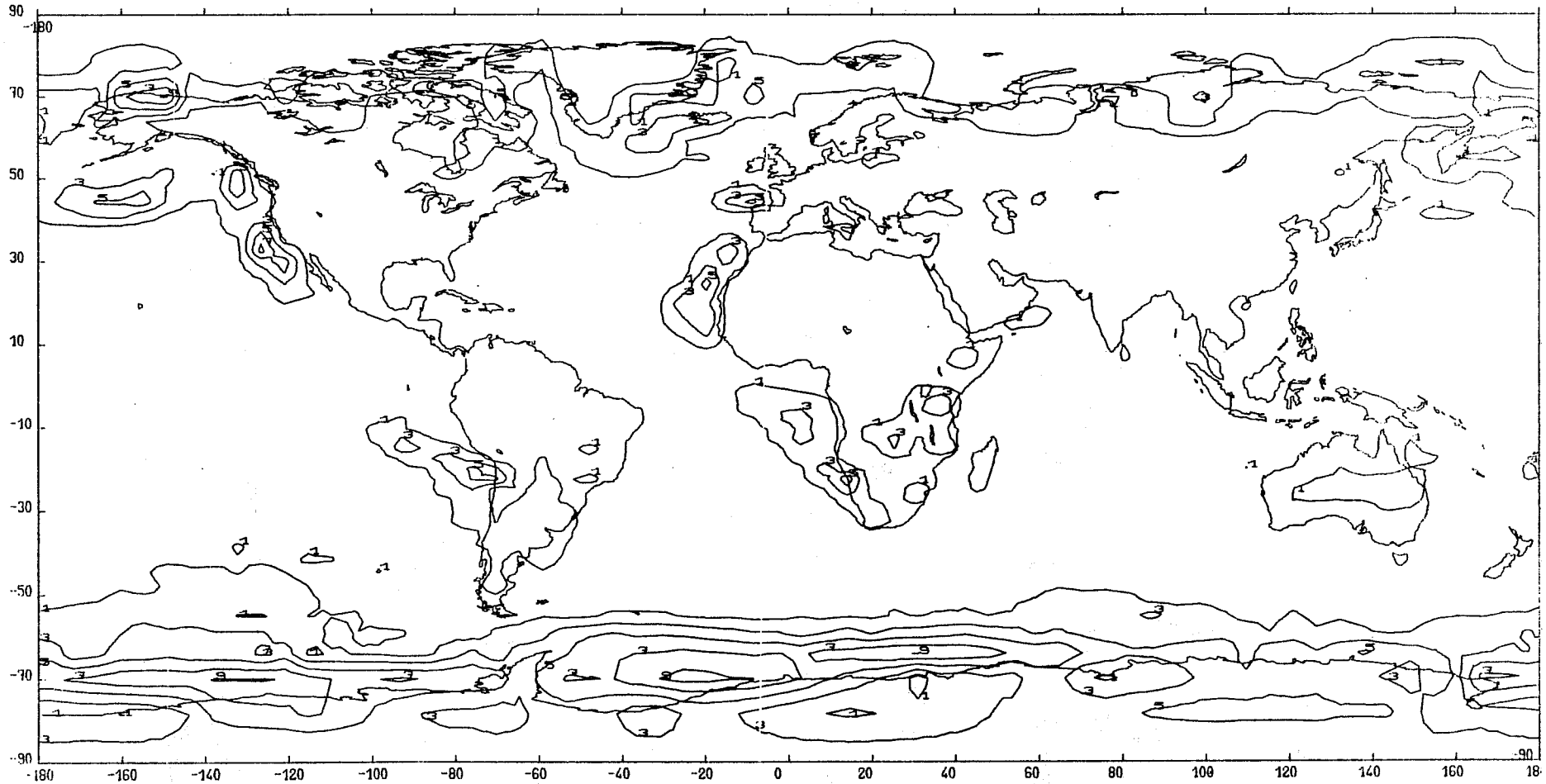

Figure 3 : Mean stratus cloud cover (days 20 to 50,STR experiment)
(values are in tenths)

The amount of predicted stratus clouds stays fairly uniform throughout the integration. We show in Figure 3 the mean stratus cloud cover between the days 20 and 50 of the integration. Again their location appears correct when compared with available climatologies.

2.3 Impact of the stratus clouds on the simulated climate

We now compare the results of the experiments CO and ST averaged over the days 20 to 50. Clearly the first impact of the stratus clouds will be on the radiative fluxes. We show in Figure 4 the planetary albedo for the experiment STR. Near the coast of California the albedo is over .3 in the STR case, whereas it is less than .2 in the CO experiment. Similar increases are found near Mauritania, the Congo and Peru. Compared with the distributions of Winston et al (1979) our values are somewhat lower, but the general pattern is correct. The changes in the net radiative fluxes at the top or at the bottom of the atmosphere (not shown here) are mainly due to this modification of the albedo. But within the atmosphere there appears a strong cooling at the cloud level which spreads throughout the troposphere and which is due to the cloud longwave emission. This is illustrated by Figure 5 where we show the differences of temperature at 850 mb between the ST case and the CO case. At subtropical latitudes there is a decrease of at least 2°C associated with the presence of the stratocumulus. In the Arctic there is also a general cooling.

The impact of the stratus clouds on the simulated climate is certainly severely diminished because we do not predict the SSTs. In particular the differences in the mean precipitation field simulated in the experiments STR and CO are within the variability of the model and do not appear to be

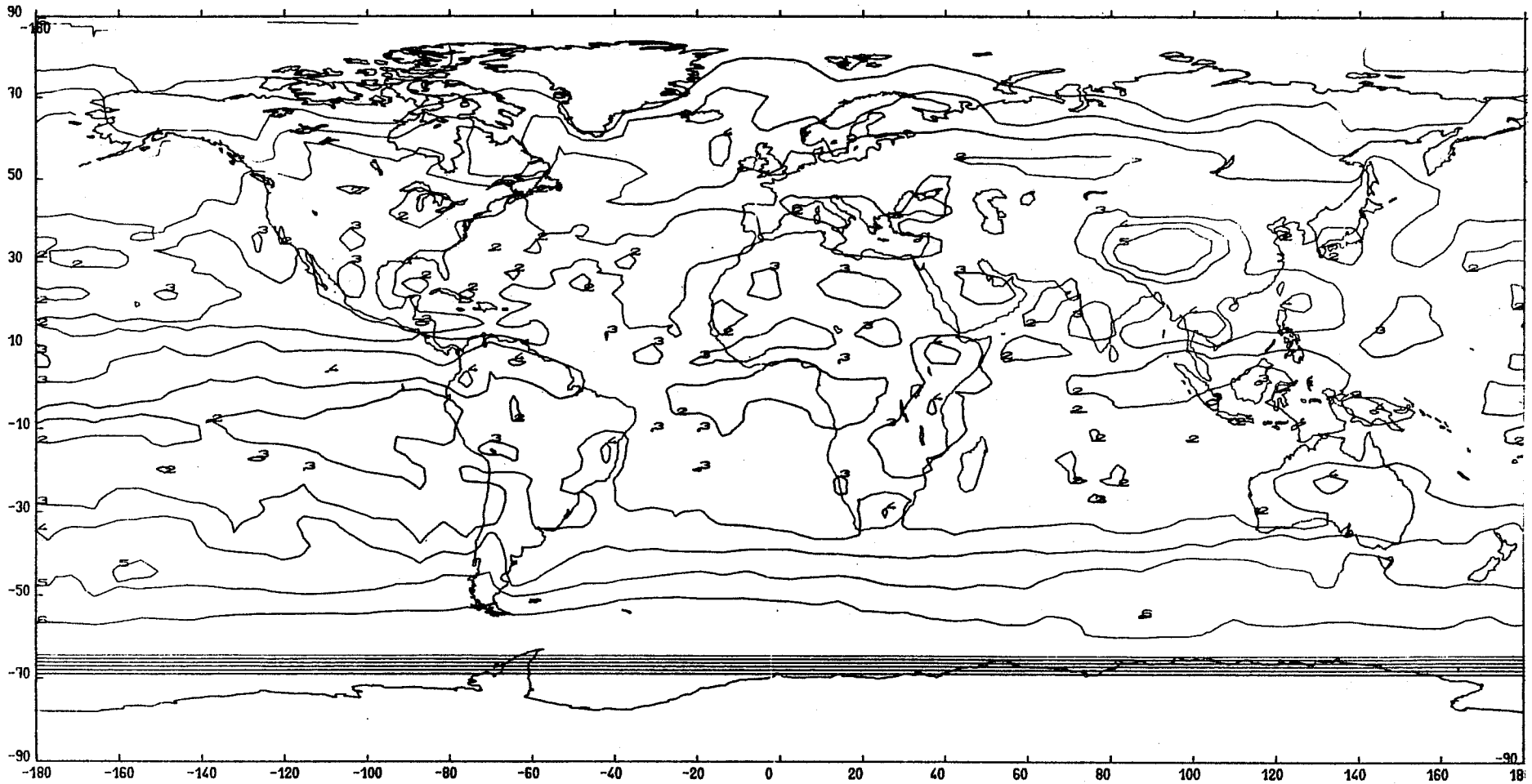

Figure 4 : Mean albedo (days 20 to 50 , STR experiment)

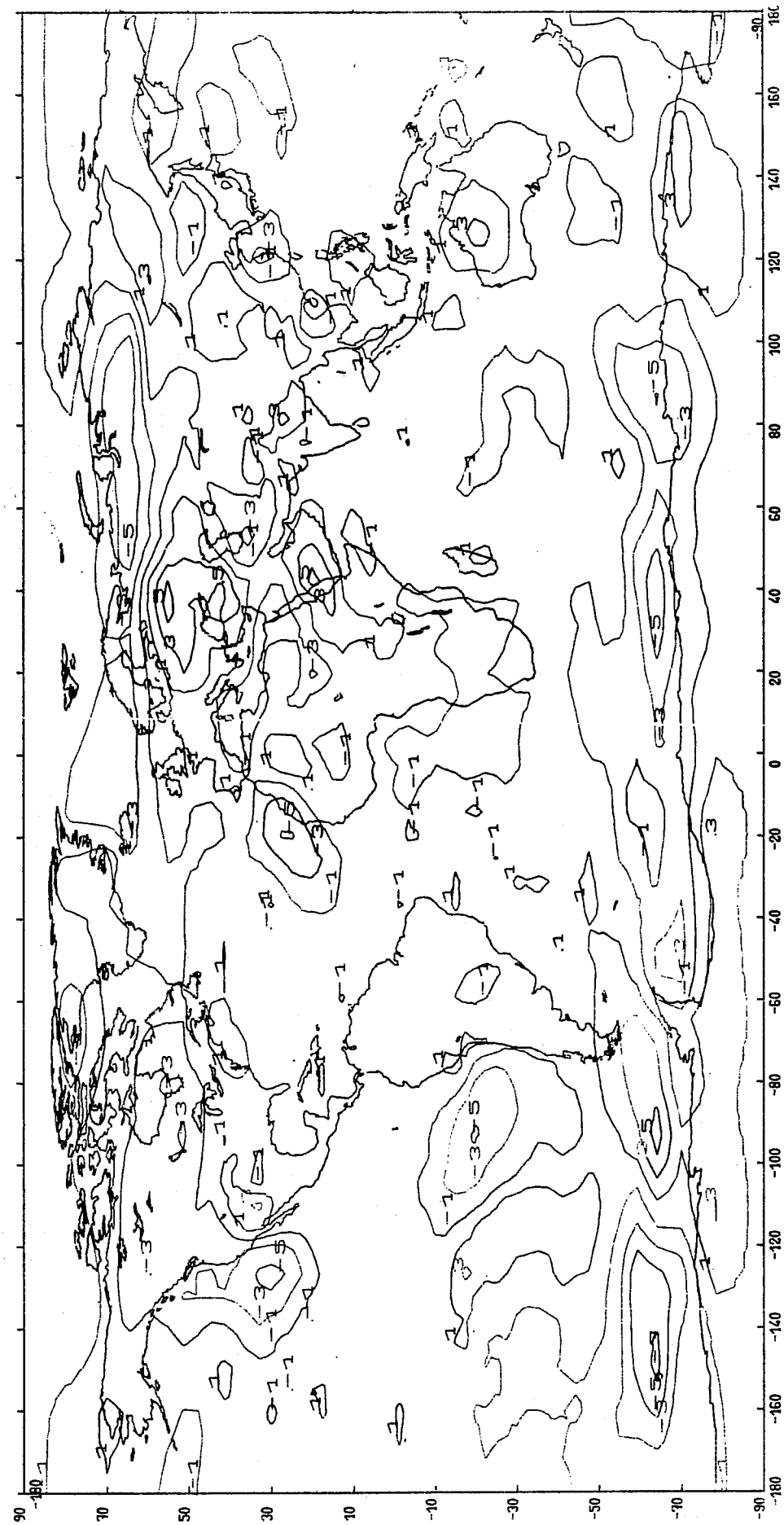

Figure 5 : Mean temperature differences at 850 mb between the STR and CO experiments
(days 20 to 50)

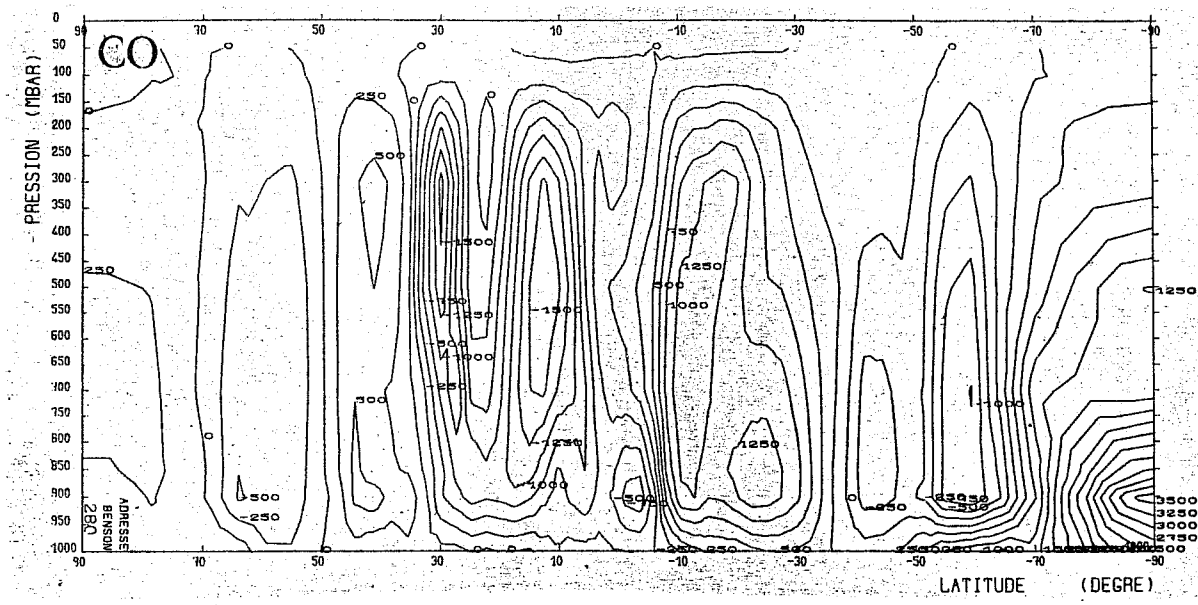

Figure 6: Mean zonal vertical velocities for the CO experiment (days 20 to 50).

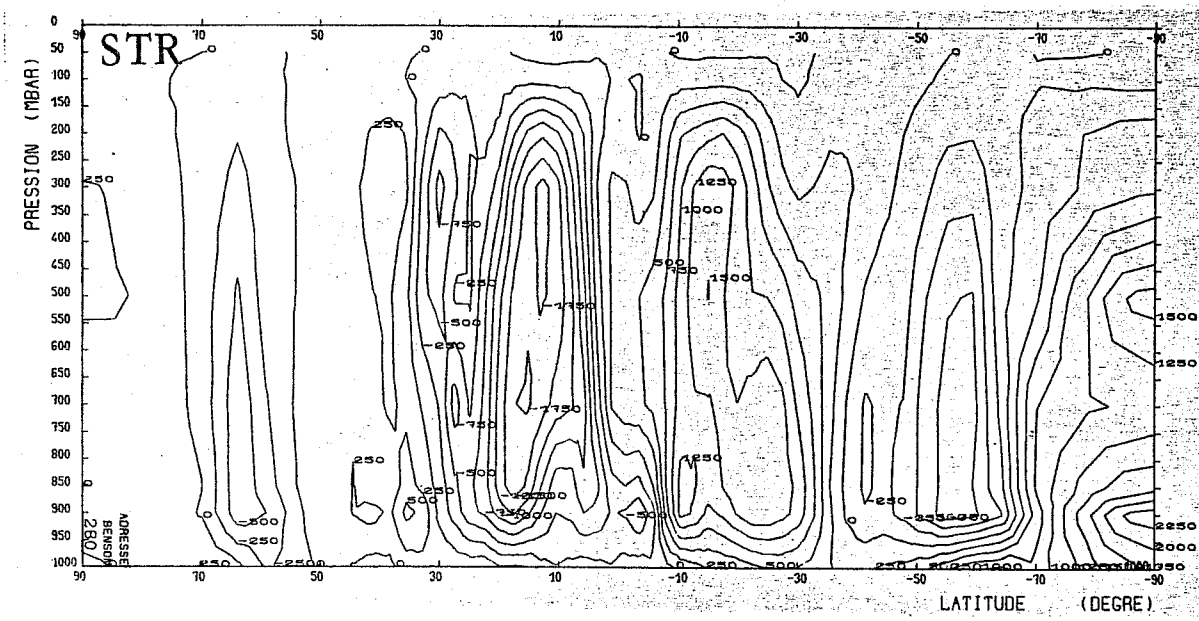

Figure 7: As Figure 6, but for experiment STR.

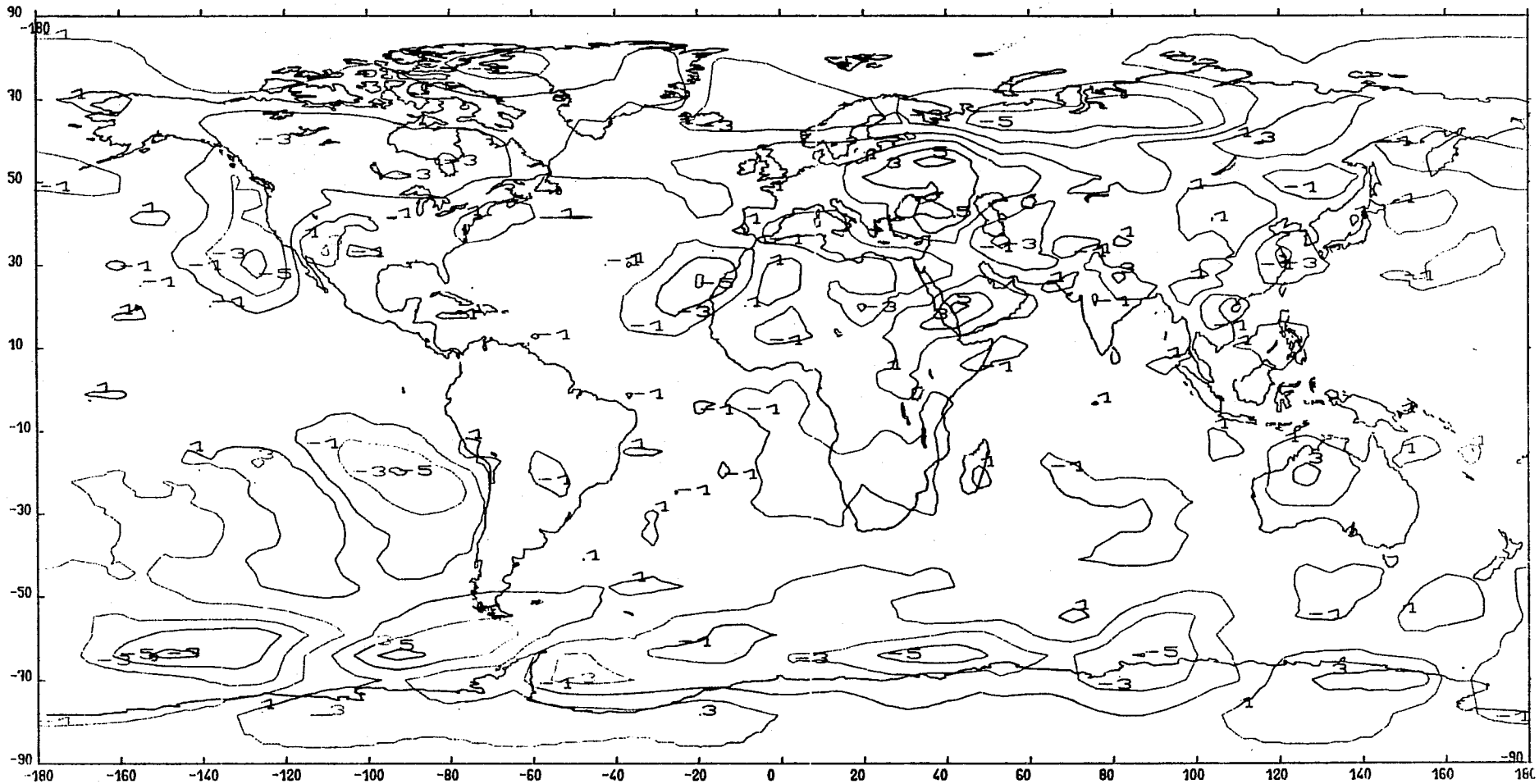

Figure 5 : Mean temperature differences at 850 mb between the STR and CO experiments (days 20 to 50)

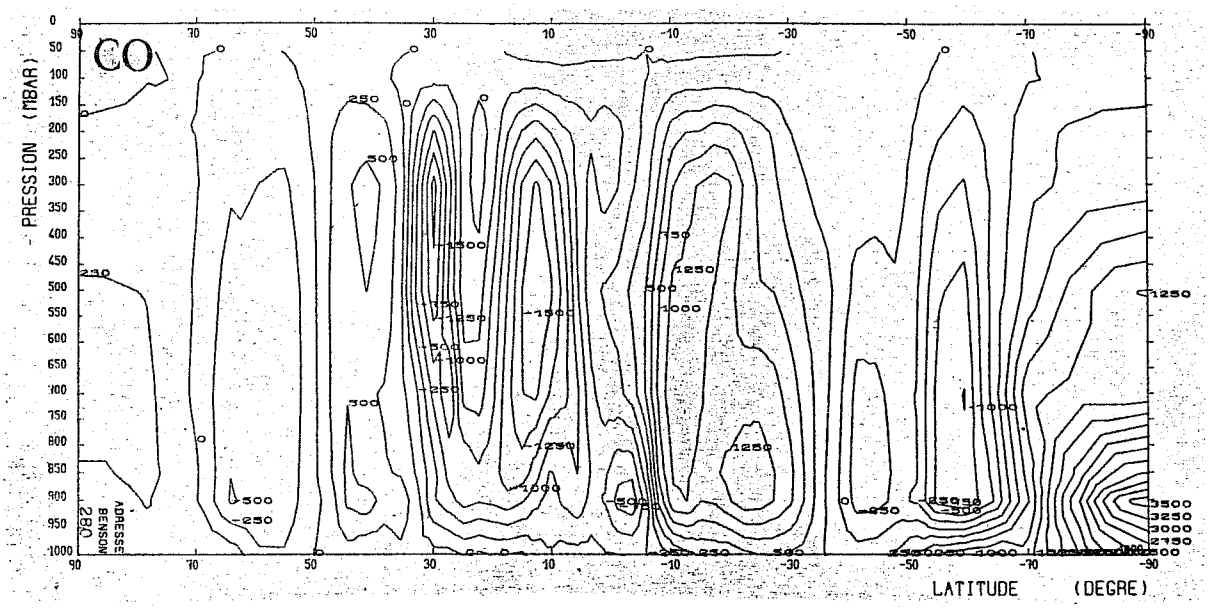

Figure 6: Mean zonal vertical velocities for the CO experiment (days 20 to 50).

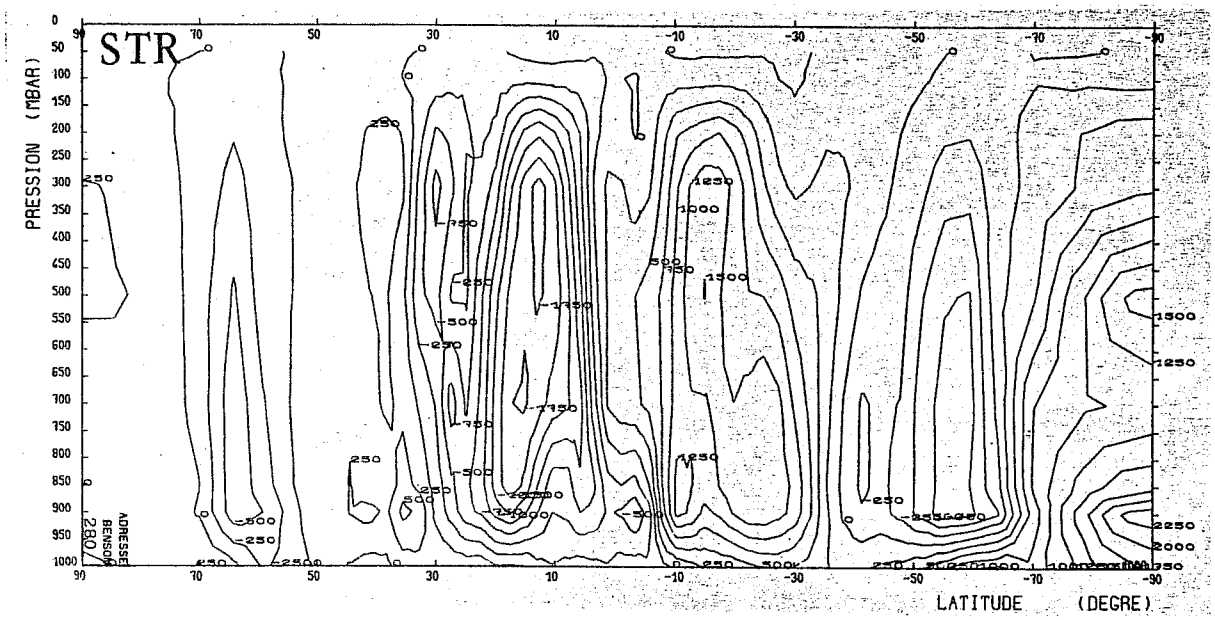

Figure 7: As Figure 6, but for experiment STR.

	transient AE		transient KE		transient conversion	
	NH	SH	NH	SH	NH	SH
STR	1.05	2.04	3.34	6.10	1.37	2.42
CO	1.02	2.21	3.83	6.78	1.24	2.52

	stationary AE		stationary KE		stationary conversion	
	NH	SH	NH	SH	NH	SH
STR	3.42	2.66	2.77	3.66	1.85	0.12
CO	3.05	2.42	2.41	3.60	1.55	0.14

Table 1 : Eddy energetics for the experiments STR and CO. The avalaible potential energy (AE) and the kinetic energy (KE) are in 10^5 J/m^2 and the conversion between the two in W/m^2.

significant. Yet the influence on the mean circulation is not negligible. In Table 1 we show analyzes of the eddy energetics of the two integrations. The differences are generally much larger than the differences found in earlier sensitivity experiments where we studied the effect of zonally averaging or time averaging the cloudiness field (Le Treut, 1983 or Laval and Le Treut, 1984). Therefore the strong enhancement of the stationary energetics which is observed in the STR case appears highly significant. We also show in Figures 6 and 7 the zonal mean of the vertical velocities for the two experiments. The STR experiment is characterized by a strong enhancement of the polar cell. Again over many experiments differing only by their cloud cover this effect appears only in the STR case and it should be attributed to the stratus cloud cover.

3. A STATISTICAL APPROACH OF NON CONVECTIVE PRECIPITATION AND CLOUDINESS

One of the crudest assumption mode in the usual version of the LMD GCM, as well as in many other GCMs, is to consider that non-convective condensation occurs only when the whole gridbox is saturated in water vapour. Statistical parameterizations have been designed either in mesoscale models (Deardorff and Sommeria (1977), Bougeault (1981) or in large scale models (Sasamori (1976), Hense and Heise (1984)) to overcome this difficulty. Sasamori's scheme for example first determines the variability of the vertical wind and then predicts the cloud fraction, the precipitation and the cloud liquid water content.

In the study described here we have used a similar but simpler approach in which we directly diagnose the internal variance Δq of the water vapour mixing ratio within a given gridbox at a given time from the variance of the mixing ratio predicted in this location during the previous six hours.

This time lapse was chosen because it was large enough compared to the dynamical time step of the model and small enough compared to the time scale of the displacement of mid-latitude cyclones. Our assumption is admittedly very crude. But the values obtained for the ratio $\frac{\Delta q}{q}$ have a reasonably physical meaning : they show a strong maximum near the tropopause at low latitudes. At low levels $\Delta q/q$ is over 10 % only in the Winter Hemisphere in cyclonic regions. Yet the variability of the mixing ratio in the PBL is probably underestimated.

We then define the cloud fraction f by the simple linear relation :

$$f = \frac{q+\Delta q-qs}{2\Delta q} \quad \text{with } 0 \leqslant f \leqslant 1.$$

The cloudy fraction f has then a mixing ratio $q_c = \frac{q+qs+\Delta q}{2}$, whereas the clear fraction (1-f) has a mixing ratio $q_{c\ell} = \frac{q+qs-\Delta q}{2}$. Precipitation occurs in the cloudy fraction through the usual procedure.

We have used this scheme for a simulation of the July climate from the same initial state and in the same conditions than the two experiments already described. This new experiment will be referenced as STA.

We first show in Figure 8 the low cloudiness simulated for the 12th of June 1979. Compared with the STR and CO experiments the main differences are over the Northern Atlantic ocean and over the Pacific ocean near 20°N. The cloud structure which appears over the Atlantic at 30°N seems consistent with the Meteosat picture for the same day.

The introduction of this parameterization modifies the proportions of

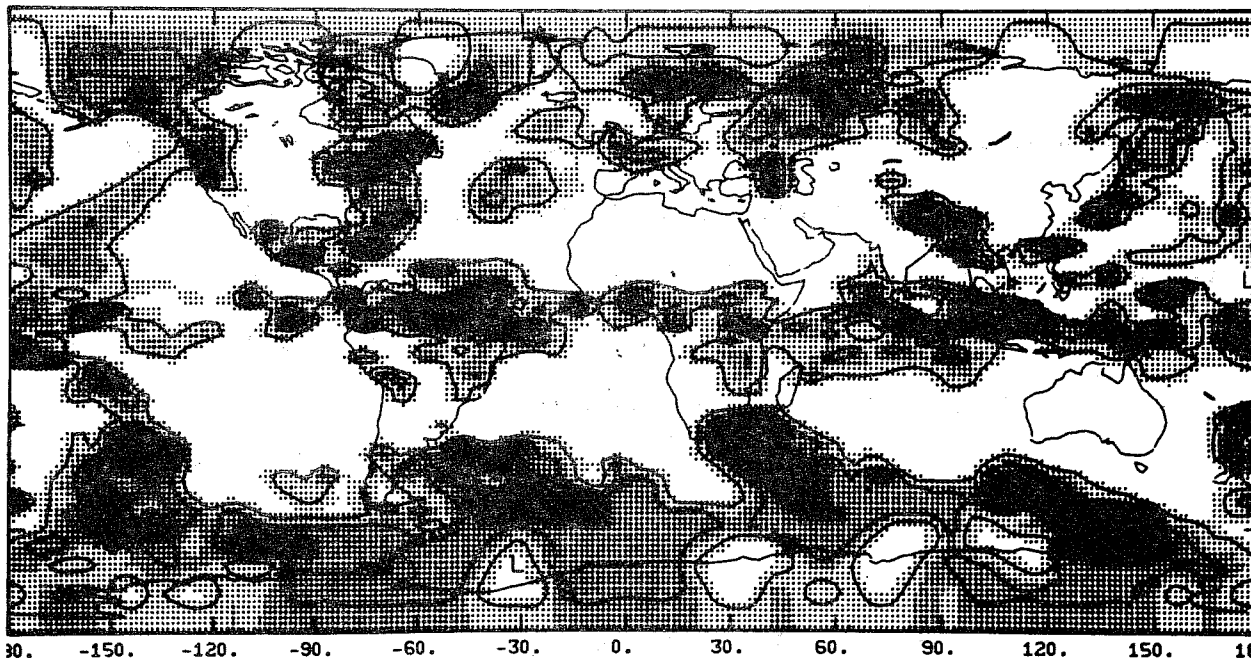

Figure 8 : Low cloudiness on the 12th of June 1979 (STA experiment)

	Ocean				Land			
days	0-10	10-20	20-30	30-40	0-10	10-20	20-30	30-40
low cloudiness								
90N-45N	.00	+.04	+.04	+.08	-.05	-.02	-.04	-.03
45N-15N	.00	.00	-.01	.00	-.02	-.01	+.01	.00
15N- 5S	-.13	-.07	-.04	-.04	-.05	-.06	-.04	-.01
5S-30S	+.02	+.10	+.05	+.08	-.01	+.03	-.02	.00
30S-60S	-.09	-.07	-.05	-.08	+.05	-.01	-.01	-.12
60S-90S	+.02	+.03	+.08	+.05	0.	0.	0.	0.
middle cloudiness								
90N-45N	.00	+.04	+.05	+.02	.00	+.01	.00	+.01
45N-15N	.00	-.01	-.01	.00	.00	+.02	+.02	+.01
15N- 5S	-.04	-.03	.00	+.02	-.01	-.02	.00	-.01
5S-30S	.00	.00	.00	+.02	.00	+.01	.00	+.02
30S-60S	+.01	-.01	-.01	+.01	+.06	+.07	+.06	+.03
60S-90S	-.11	-.12	-.11	-.12	0.	0.	0.	0.
high cloudiness								
90N-45N	-.07	-.12	-.21	-.22	-.03	-.11	-.11	-.11
45N-15N	-.10	-.17	-.16	-.13	-.16	-.18	-.15	-.20
15N- 5S	-.11	-.14	-.15	-.22	-.10	-.16	-.23	-.25
5S-30S	-.11	-.18	-.17	-.15	-.13	-.18	-.24	-.20
30S-60S	-.07	-.13	-.16	-.14	-.06	-.10	-.26	-.13
60S-90S	-.31	-.37	-.42	-.40	0.	0.	0.	0.

Table 2 : Cloudiness statistics (differences between the experiments STA and CO ,zonal averages given for 10-days periods and for 6 latitude bands)

days	0-10	10-20	20-30	30-40
Non convective precipitation (cm/year)	22.4	24.2	22.1	25.2
Convective precipitation (cm/year)	-19.2	-21.3	-13.6	-15.0
Solar radiative flux (W/m^2)				
top of the model	8.1	7.1	8.0	7.1
bottom of the model	8.1	6.6	7.5	6.6
Downward infrared flux (W/m^2)				
top of the model	5.3	6.5	6.9	8.1
bottom of the model	3.5	1.9	2.3	2.4

Table 3 : Global statistics: differences between the experiments STA and CO for 10-days periods

convective and the non-convective precipitation. Moreover it tends to dry out the atmosphere. This explains why the comparison between the STA and CO experiments will give different results when performed at the beginning of the experiment or on climate means. To have a better insight into our results we have displayed in Table 2 and Table 3 the differences between STA and CO for statistics about cloudiness, precipitation or radiation, averaged over 4 successive ten-days periods.

The main feature is a clear reduction of the high cloudiness, which does not exist on the first day, but then develops quickly. Another important effect is the sharp reduction of the middle and high cloudiness near the Pole in the Winter Hemisphere. At low levels we may note a reduction of the convective cloudiness over the ocean in the region of the ITCZ and an increase of the cloud cover over the oceans, at subtropical latitudes in the Southern Hemisphere, and near the Poles. On the whole the total amount of cloudiness tends to decrease, which may be seen by the increase of the net downward solar radiation. But at the same time the precipitation increases because the decrease in convective precipitation is not enough to balance the increase of the non-convective precipitation.

The response of the model to this new parameterization is of an intricate nature and has to be considered with caution. In particular it should depend critically on the convective schemes used in the model (in the LMD GCM we use both a Kuo-type scheme and a moist adiabatic adjustment (MAA) scheme which were kept unchanged) and on the representation of the convective cloud cover (we predict 100 % cloudiness whenever the MAA occurs, and a fractional value for the two-type scheme). Yet the effects are important enough to deserve further studies.

4. PREDICTION OF THE CLOUD LIQUID WATER CONTENT

Predicting the cloud liquid water content as a new prognostic variable of the GCMs is certainly a necessity, particularly in the perspective of predicting the optical properties of the simulated clouds. Yet there has been until now few attempts to do it, the only published study being that of Sundqvist (1981). We have started a project with such an objective in mind but as only preliminary results are available, we will mainly give in this section a brief description of the difficulties we have met, and of our objectives for the future.

We want to parameterize the sources, the transport and the sinks of the cloud liquid water. As far as the sources are concerned the main problem arises because,in the usual parameterisations of the convection, only the total amount of the condensed water is determined but its vertical distribution remains unknown. Designing a convective scheme in which the cloud liquid water content as well as its entrainment would be taken explicitely into account is certainly an important task. For the moment we have chosen a simple approach where the vertical distribution of the cloud water is chosen to be proportional to that of the heating. Problems in transporting the liquid water arise because this variable is both discontinuous and positive, and in a grid point model as the LMD GCM the choice of a discretization for the term $\vec{\nabla}(\vec{V}q_\ell)$ is a difficult problem.

The sinks of the cloud liquid water are of two kinds : the reevaporation of the cloud droplets and their conversion into precipitating droplets. This second mechanism is specially difficult to parameterize in a general circulation model. Mesoscale models already includes such a physics and many of them use the parameterization of Kessler (1969). Kessler represented

two mechanisms : the autoconversion of the cloud dropplets, which depends on a critical threshold a on the liquid water mixing ratio, the value $a = 5.10^{-4}$ being often chosen, and the collection of the cloud dropplets by the precipitating droplets. Sundqvist (1978) represents those phenomenon by a formula relating the precipitation rate to the cloud water content. To begin with we chose an even simpler approach and we simply allowed all the water beyond the critical parameter a to rain out, this being done every 30 minutes, and we integrated the model for 10 days starting from the 11th of June 1979. During this period no equilibrium was reached : the liquid water kept increasing, especially in the polar regions and in the upper layers of the model. Few data concerning the global field of cloud liquid water are available, but the studies of Prabhakara et al (1983) derived from Nimbus 7 or those of Matveev (1984) derived from Cosmos 243 give the same order of magnitude, with a maximum of about 410^{-2} g cm^{-2} in the Tropics. Our results were much higher.

Several reasons may be invoked to explain it : the arbitrary value for the threshold a, and also it may be that, following Mason (1971), the mechanisms of precipitation of the clouds whose top is approximately below -10°C are very different because of the presence of ice crystals. We have rerun our experiment with a lower threshold, $a = 10^{-4}$, and allowed the cold top clouds to rain out almost completely. The global field of cloud liquid water after five days is shown in Figure 9. At this time the global amount of cloud liquid water has reached an equilibrium, and the values obtained, as well as the general pattern, are qualitatively correct.

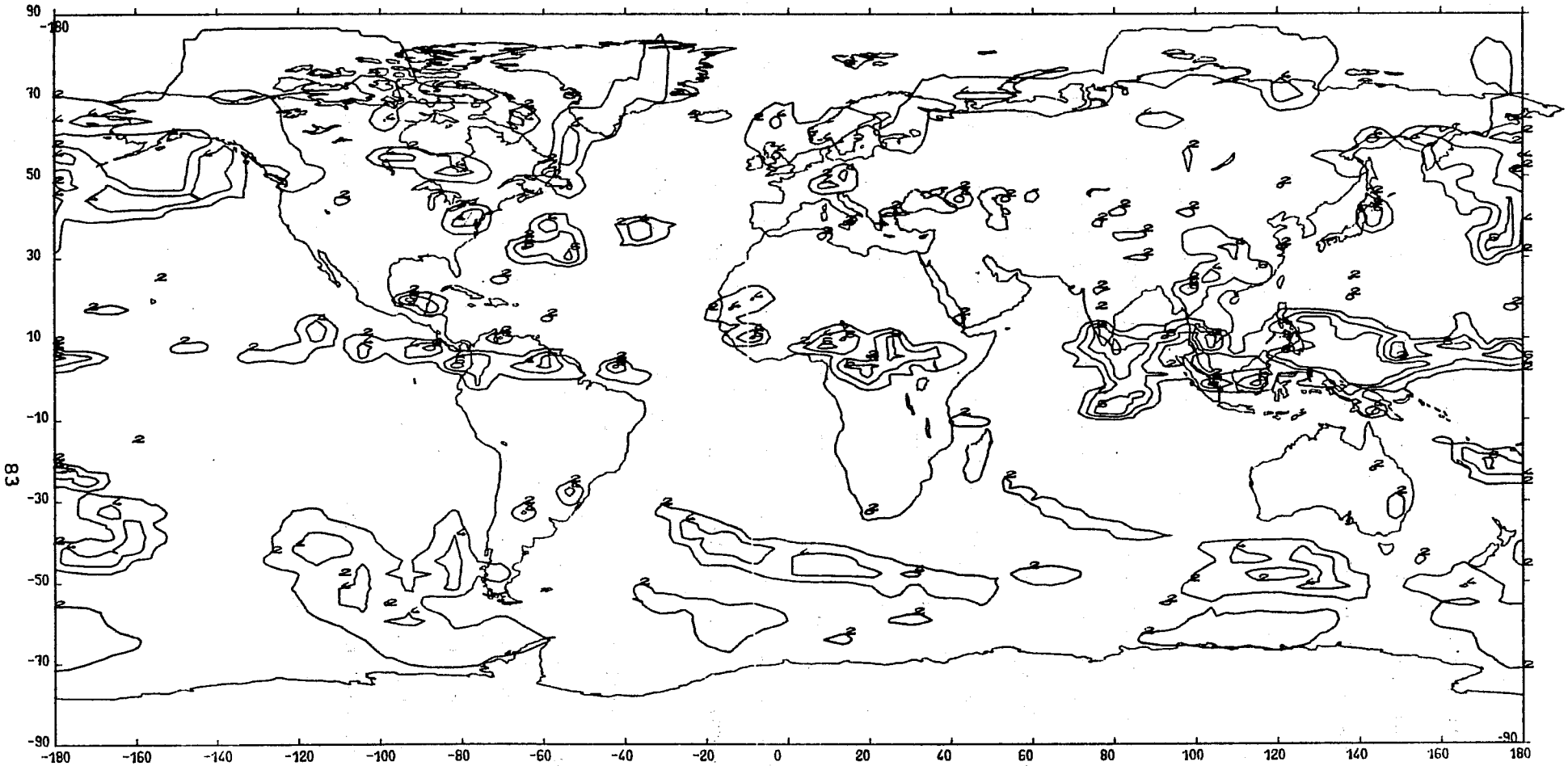

Figure 9 : Cloud liquid water content after 5 days of integrations of the model (the interval between two isolignes is 2. 10^{-2} g/cm^2)

In conclusion there remains much work to be done in order to include in a proper way the cloud microphysics in our GCM. But the results presented here suggest that this is a reasonable objective.

5. CONCLUSION

When analyzing these results it is important to keep in mind that cloudiness is one of the GCM outputs which depends most on the model formulation, on its resolution, both horizontal and vertical, on the representation of the water vapour transport, on the parameterization of the convection. Moreover the cloud modellers are presently faced with the difficult problem of validating their results.

Our approach in trying to develop an interactive GCM for climate studies is therefore the following : we first test the sensitivity of the model to the various simplicities of its cloud parameterization and we then try to develop a model where there will be a greater physical consistency between the representation of the cloud cover and that of the hydrological cycle. There remains many problems to be solved. One of the most important, although not treated here, may be the representation of the convective cloud cover in the Tropics. But on the whole the results shown here are encouraging and we hope that, by the time the ISCCP data will become available, the cloud models that they will serve to validate will have a stronger physical basis than they have now.

6. REFERENCES

Bougeault, Ph., 1981a : Modeling the trade-wind cumulus boundary layer. Part I : Testing the ensemble cloud relations against numerical data. J. Atmos. Sci., 38, 2414-2428.

Bougeault, Ph., 1981b : Modeling the trade-wind cumulus boundary layer. Part II : A high order one dimensional model. J. Atmos. Sci., 38, 2429-2439.

Deardorff, J.W., and G. Sommeria, 1977 : Subgrid-scale condensation in models of nonprecipitating clouds. J.Atmos. Sci., 34, 344-355.

Hense, A. and E. Heise, 1984 : A sensitivity Study of Cloud Parameterizations in General Circulation Models, Beitr. Phys. Atmosph., 57, pp. 240-258.

Laval, K. and Le Treut, H., 1984 : The influence of cloud radiation interaction on the simulation of the climate by a general circulation model, in preparation.

Le Treut, H., 1983 : Sensitivity studies of GCM simulations to cloudiness specification. ECMWF Workshop on Convection in Large-Scale models, October 1983.

Le Treut, H. and K. Laval, 1984 : The importance of cloud radiation interaction for the simulation of climate, in New Perspectives in Climate Modelling, edited by Berger and Nicolis, Elsevier Publishing Company - Amsterdam.

Lilly, D.K., 1968 : Models of cloud-topped mixed layers under a strong inversion, Quart. J. Roy. Met. Soc., 105, 303-306.

Mason, B.J., 1971 : The Physics of clouds, Clarendon Press - Oxford, pp. 280-368.

Matveev, L.T., 1984 : Cloud dynamics, Reidel Publishing Company - Dordrecht, pp. 116-136.

Ramanathan, V., and R.E. Dickinson, 1981 : A scheme for forming nonprecipitating low level clouds in GCMs. Clouds and Climate, Report of Workshop held at NASA Goddard Inst. for Space Studies, Oct. 29-31, 1980, pp. 85-87.

Prabhakara, C., T. Wang, A.T.C. Chang and P. Gloersen, 1983 : A statistical examination of Nimbus 7 SMMR Data and Remote Sensing of Sea-Surface Temperature, Liquid Water Content in the Atmosphere and Surface Wind Speed, J. Clim. Applied Meteor., 22, 2023-2037.

Sadourny, R. and K. Laval, 1984 : January and July performance of the LMD GCM, in New Perspectives in Climate Modelling, edited by Berger and Nicolis, Elsevier Publishing Company - Amsterdam.

Sasamori, T., 1975 : A Statistical Model for Stationary Atmospheric Cloudiness, Liquid Content and Rate of Precipitation, Mon. Wea. Rev., 12, 1037-1049.

Slingo, J.M., 1980 : A cloud parameterization scheme derived from GATE data for use with a numerical model. Quart. J. Roy. Met. Soc., 106, 747-770.

Suarez, M.J., A. Arakawa, and D.A. Randall, 1983 : The parameterization of the planetary boundary layer in the UCLA general circulation model : Formulation and results. Mon. Wea. Rev., (to appear).

Sundqvist, H., 1978 : A parameterization scheme for non-convective condensation including prediction of cloud water content. Quart. J. Roy. Met. Soc., 104, 677-690.

Sundqvist, H., 1981 : Prediction of stratiform clouds : Results from a 5-day forecast with a global model. Tellus, 33, 242-253.

Winston, J.S., A. Gruber, T.I. Gray, M.S. Varnadore, C.L. Earnest, and L.P. Mannello, 1979 : Earth-Atmosphere Radiation Budget Analyses Derived from NOAA Satellite Data, U.S.A Department of Commerce, NOAA.